THE ASTROPHYSICAL JOURNAL, 298:95–106, 1985 November 1

THE OPTICAL STRUCTURE OF X-RAY GLOBULAR CLUSTERS

PAUL HERTZ[1]
E. O. Hulburt Center for Space Research, Naval Research Laboratory
AND
JONATHAN E. GRINDLAY[2]
Harvard-Smithsonian Center for Astrophysics
Received 1984 November 19; accepted 1985 May 2

ABSTRACT

We have obtained CTIO 4 m prime-focus plates of eight globular clusters containing bright X-ray sources. Plates in several colors (principally U and B) of each cluster have been digitized. A maximum symmetry method for determining the center of a globular cluster image is described and applied to each cluster in order to determine the cluster center with an accuracy of $\sim 1\farcs0$. Surface brightness profiles have been derived for seven clusters and fitted with King models to yield core radii within $\sim 10\%$. These determinations of the cluster centers and core radii are sufficiently accurate to allow Grindlay *et al.* to statistically measure the mass of the globular cluster X-ray sources. Two clusters (NGC 6624 and M15) show significant excesses of light in their cores over the best-fit King model, in agreement with the results of Djorgovski and King. The significance of these excesses, as well as the lack of any dependence of globular cluster structural parameters on color, is discussed.

Subject headings: clusters: globular — stars: stellar dynamics — X-rays: sources

I. INTRODUCTION

X-ray globular clusters, those galactic globular clusters containing bright X-ray sources, have drawn considerable interest since the discovery of globular cluster X-ray sources (see Hertz 1984 for a recent review). The answers to such fundamental questions as the formation, evolution, and physical nature of the X-ray sources seem to depend on the properties of the globular clusters themselves. Soon after the identification of the first X-ray globular clusters (Giacconi *et al.* 1974), it was noted that these clusters are more centrally concentrated and have shorter relaxation time scales than the average cluster (Clark 1975; Bahcall and Ostriker 1975; Bahcall and Hausman 1976). Recently it has been noted that the existence of a high-luminosity globular cluster X-ray source is correlated with a cluster's galactocentric distance (Lightman and Grindlay 1982) and that the existence of both high- and low-luminosity X-ray sources is correlated with the cluster's time scale for binary formation via the tidal capture mechanism (Lightman and Grindlay 1982; Hertz and Grindlay 1983; Hertz and Wood 1985).

The study reported here was prompted by the realization that the location of an X-ray source within a globular cluster's potential well allows a statistical determination of the mass of the X-ray system (Bahcall and Wolf 1976). Lightman, Hertz, and Grindlay (1980) have shown that this mass can be derived only when

$$\sigma_t < r_c(3q - 1)^{-1/2} , \quad (1)$$

where r_c is the cluster core radius, q is the ratio of the mass of the X-ray system to the mean stellar mass in the cluster core, and σ_t is the total uncertainty in the determination of the X-ray source position, cluster center, and core radius. Since r_c is typically $\lesssim 10''$ for X-ray globular clusters and q is as small as 2–5 if globular cluster X-ray sources are low-mass X-ray binaries (cf. Lewin and Joss 1981, 1983), the positions of the X-ray source and cluster center need to be measured to $\sim 1''$ each, and the core radius needs to be determined to $\sim 10\%$. We have met these criteria, and Grindlay *et al.* (1984) have used the precise ($\sim 1''$ uncertainty) X-ray positions measured with the *Einstein Observatory* and the cluster centers and core radii presented here to determine that q lies between 1.8 and 3.8 (90% confidence limits).

We report here initial studies of eight of the nine X-ray brightest globular clusters. (The obscured X-ray globular cluster Grindlay 1 has been observed only in the infrared [Grindlay and Hertz 1981], and its optical structure has not yet been investigated.) These studies were carried out independently of (and in advance of—cf. Grindlay 1983) the similar work recently reported by Djorgovski and King (1984, hereafter DK). We have developed and used a maximum-symmetry method (§ IIe) to determine the dynamical centers of the X-ray globular clusters by applying it to digitized images of those clusters. These images have been used to obtain accurate measurements of the clusters' core radii and to search for departures from simple King models. Motivated by the indications of approximately cusplike features in M15 (= NGC 7078; Newell, Da Costa, and Norris 1976) and, possibly, NGC 6624 (Canizares *et al.* 1978), we have analyzed each of the clusters in detail. Our analysis shows that, relative to the best-fitting single-mass King models, these two clusters really do have excess light features (cusps) and that these are almost certainly dynamically significant, since they are located at the precise cluster centers. We also find no evidence for color differences in globular cluster core radii, although our study is sensitive enough to detect any such differences.

[1] NRC–NRL Cooperative Research Associate.
[2] Visiting Astronomer, Cerro Tololo Inter-American Observatory, which is operated by the Association of Universities for Research in Astronomy, Inc., under contract with the National Science Foundation.

TABLE 1

PLATE MATERIAL FOR GLOBULAR CLUSTER STUDY

GLOBULAR CLUSTER	PLATE	COLOR	EXPOSURE	PLATE CENTER R.A.	PLATE CENTER Decl.	DATE OF PLATE
NGC 104 = 47 Tuc	4213	*B*	3 min	$00^h21^m52^s$	$-72°21''33''$	1979 May 25/26
	4224	*U*	1 min	00 21 45	−72 21 51	1979 May 27/28
NGC 1851	5344	*B*	30 s	05 13 18	−40 04 22	1981 Sep 29/30
	5345	*U*	10 min	05 13 18	−40 04 22	1981 Sep 29/30
Terzan 2	3277	*I*	60 min	17 22 50	−30 31 30	1977 Aug 24/25
Liller 1	3288	*I*	60 min	17 31 07	−33 34 50	1977 Aug 25/26
NGC 6441	4199	*B*	30 s	17 46 48	−37 02 17	1979 May 25/26
	4200	*U*	15 min	17 46 48	−37 02 17	1979 May 25/26
NGC 6624	4205	*B*	30 s	18 20 28	−30 23 14	1979 May 25/26
	4206	*U*	15 min	18 20 28	−30 23 14	1979 May 25/26
NGC 6712	4210	*B*	6 min	18 50 23	−08 45 36	1979 May 25/26
	4216	*U*	29 min	18 50 21	−08 46 06	1979 May 26/27
	4217	*U*	35 min	18 50 21	−08 46 06	1979 May 26/27
NGC 7078 = M15	5347	*B*	30 s	21 28 46	+12 03 35	1981 Sep 30/Oct 1
	5334	*U*	8 min	21 28 46	+12 03 35	1981 Sep 29/30

NOTE.—*U* plates are on IIIa-J emulsion through a UG-2 filter; *B* plates are on IIIa-J emulsion through a GG-385 filter. Both *U* and *B* plates were baked in forming gas according to standard CTIO procedures. The *I* plates are on IV-N emulsion through a RG-695 filter and were sensitized in a 1.9% $AgNO_3$ bath.

II. DATA AND METHODOLOGY

We have obtained (during observing runs in 1977–1981) CTIO 4 m prime-focus plates in several colors (primarily *U* and *B*) of the eight globular clusters in this study. The Photometric Data System (PDS) microdensitometers at Princeton Observatory and Yale University have been used to digitize the relevant areas of these plates. Using the sensitometer spot data recorded on each plate, the characteristic density-intensity curve is calibrated and applied to the data. Single-mass King (1966*a*) models of globular clusters were fitted to the digital data, and the structural parameters of the model clusters were varied until the best fits were obtained. In this manner we determined the location of the centers of the globular clusters, the core radii, and, in some instances, indications of the tidal radii or concentration parameters.

a) Choice of Plate Material

Whenever possible, two 4 m plates of each cluster in different colors were chosen for digitizing. As has been noted (e.g., King 1980; DK), *U* plates are needed to minimize the contribution of individual cluster stars to the photographic surface brightness profile of the globular cluster, especially within the inner 5″ of the core. Since no significant differences are observed between the two colors (see § V), final results are based on averages of the results for each plate analyzed. We have chosen exposures that are deep enough to allow determination of the surface brightness profile to $\gtrsim 10r_c$ but are not so deep as to overexpose the cluster core. Our plates are thus insenstive to the tidal radius or cluster concentration parameter. The plates analyzed, and some relevant characteristics, are shown in Table 1.

b) Digitization of Photographic Images

The CTIO 4 m (prime-focus) plates are $\sim 1°$ (diameter) fields centered on the cluster. The area digitized include the sensitometer spots, the image of the globular cluster, images of stars chosen as secondary astometric standards, and a quick scan of the entire plate to determine the plate background. Each of these scans was performed with diffierent scan parameters (see Table 2). The plate scale of a prime-focus 4 m plate is 53.6 μm arcsec^{-1}.

c) Astrometry

Precise measurements of the cluster center depend on accurate astrometric calibration of the plate. Stars from the *SAO Star Catalogue* (1966) located near the globular clusters and visible on the appropriate sky survey plate (either the Palomar Observatory Sky Survey red prints or the European Southern Observatory "Quick Blue" Survey plates) were used as primary astrometric standards. Secondary astrometric standards were chosen from stars visible on both the 4 m program plates and the sky survey plates. The celestial coordinates of the secondary standards were measured from the sky survey plates with the Center for Astrophysics measuring engine to an accuracy of $\lesssim 0''.5$. This accuracy was obtained by repeating measurements 6–12 times, including rotation of the survey plate between measurements and use of a varying group of 10–15 primary standards. The 5–13 secondary standards for each 4 m program plate were raster-scanned, and the digitized images were processed using the maximum-symmetry method (described below). The location of each secondary standard in plate coordinates was determined to $\lesssim 25$ μm, or $\lesssim 0''.5$ on the sky.

In Table 3 we give the astrometric precision which we were able to obtain for each cluster. The uncertainty in a single star's position is the rms scatter of the secondary standards about the best-fit coordinate system on the digitized 4 m program plates. The uncertainty in a plate's coordinate system is the uncer-

TABLE 2

PARAMETERS FOR PDS SCANNING OF PLATE MATERIAL

Feature Scanned	Square Aperture Size (μm)	Raster Step Size (μm)	Number of Steps
Sensitometer spots	50	50	50 × 50
Secondary standards	20	10	50 × 50
Cluster core	50	25	400 × 400
Cluster	50	250	400 × 400
Cluster halo[a]	50	250	200 × 800
Plate background	50	1000	100 × 100

[a] 47 Tuc (NGC 104) and NGC 6712 only.

TABLE 3

ASTROMETRIC ACCURACY

Globular Cluster	Number of Secondary Astrometric Standards	1 σ Uncertainty per Star (arcsec)	1 σ Uncertainty for the Plate (arcsec)
47 Tuc = NGC 104	10	2.5	~1.0
NGC 1851	13	0.8	<0.5
Terzan 2	5	1.0	~0.5
Liller 1	5	1.0	~0.5
NGC 6441	6	0.4	<0.5
NGC 6624	7	0.4	<0.5
NGC 6712	8	0.5	<0.5
M15 = NGC 7078	11	0.7	<0.5

tainty per star divided by the square root of the number of stars; we have assumed a minimum of 0".5 in this quantity to represent the fundamental limitations of using a non-astrometric catalog (i.e., the *SAO Catalogue*) for our primary standards. The uncertainties in the absolute positions for individual stars are larger than average for several clusters. The image of Liller 1 is near the edge of an ESO plate; this made measuring the position of the secondary standards difficult and subject to some systematic errors. For both Liller 1 and Terzan 2, there were problems in identifying secondary standards on both the 4 m *I* plate and the ESO *B* plate. The positions of SAO stars near the south celestial pole are poorly determined; this introduced moderate (~2".5) uncertainties into the positions of the secondary standards near 47 Tuc (= NGC 104).

d) Photographic Photometry

The 50 × 50 raster of each sensitometer spot yielded 2500 samples of the density of the emulsion in the spot. The sensitometer spot data was fitted to the known relative intensity of the light illuminating each spot during exposure (Schweizer, Gonzalez, and Saa 1980); the seven-parameter curves of Tsubaki and Engvold (1975) were used. The fits were good for all plates, and the average scatter in intensity about the best-fit characteristic curve was <5% for each spot. In order to estimate the measurement error for a single measurement in the raster scans of the cluster, the measured scatter in the 2500 samples of each sensitometer spot was used as an estimate of the uncertainty in a single measurement at the density of the spot. A power law ($\sigma_d \propto d^{\alpha}$) was fitted to the data and used to estimate the measurement errors of all subsequent density measurements.

A background scan of each plate was used to determine large-scale nonuniformities and fogging in the plate emulsion. A background scan of the entire plate was made with ~1 mm resolution, the cluster and obvious stars were removed, and a two-dimensional linear function was fitted to the remaining $\sim 5 \times 10^3$ pixels. The difference between the background density at any point on the plate and the background density at the sensitometer spots (taken as clear plate) is attributed to plate fogging and subtracted from each pixel of the cluster image.

e) The Maximum-Symmetry Method and Determination of the Cluster Center

Either two or (in the cases of the larger clusters 47 Tuc and NGC 6712) four scans are made of the cluster image on each plate. These density maps are transformed into intensity maps for further processing, and statistical and systematic uncertainties are associated with each pixel in the intensity map.

Before the image of the cluster is analyzed to determine the cluster center, the contribution of singularly bright individual stars to the image must be minimized. We have developed two schemes for accomplishing this; they yield comparable results. First, the bright stars may be identified by visual inspection of the cluster image. Pixels in the stellar images are then set equal to the mean intensity of the surrounding pixels. This is the method which we have utilized to determine the cluster centers reported in § III. Alternatively, a two-dimensional fast Fourier transform (FFT) of the cluster image may be performed, the high-frequency quadrant of the resulting power spectrum truncated, and the inverse transform applied to yield a smoothed image. We have used the FFT to study the central region of NGC 6624, as described in § IV.

The maximum-symmetry method (MSM) is used to determine the center of symmetric images. We use it to find the center of both stellar images and globular cluster images. The MSM is actually two crossed one-dimensional autocorrelations which de-weight large spikes in the data (e.g., bright stars in the cluster image) and is dominated by large-scale trends in the data (e.g., the shoulder of the cluster image). When applied to images with some symmetry, MSM yields the same center as a two-dimensional autocorrelation (such as that used by DK).

MSM entails folding a digitized image about an axis parallel to one of its edges and running through the image. The absolute differences of pixels symmetrically located with respect to the axis are summed; this yields the measure of symmetry Ψ. Let $I_{i,j}$ represent the data in pixel (i, j). The measure of symmetry Ψ about the axis $\hat{\imath}$ is then

$$\Psi(\hat{\imath}) = \Sigma_j \Sigma_i | I_{\hat{\imath}-i,j} - I_{\hat{\imath}+i,j} | , \quad (2)$$

where i is summed over half the width of the folding window and j is summed over the entire length of the folding window. The measure of symmetry Ψ is minimized when the axis of symmetry passes through the center of symmetry, and for a perfectly symmetric image Ψ vanishes. MSM is performed independently with two perpendicular sets of axes, which in practice were aligned with right ascension and declination.

An analytic approximation to a folded King model is fitted to Ψ to determine the location of its minimum. If the cluster intensity is described by the function $f(x, y)$, then the theoretical measure of symmetry $\Psi_{\rm mod}$ is

$$\Psi_{\rm mod}(\hat{x}) = \int_{-W}^{+W} dy \int_{0}^{+W} dx | f(\hat{x} - x, y) - f(\hat{x} + x, y) | , \quad (3)$$

where W is the window half-width. The folding windows used for the globular clusters in this study had half-widths of 30", with the exception of 47 Tuc (60") and NGC 6712 (120"). The

following approximations for the theoretical intensity distribution of the globular cluster images are made: first, that

$$f(x, y) \propto [1 + (r/r_c)^2]^{-1} + \text{background} , \quad (4)$$

where $r^2 = (x - x_0)^2 + (y - y_0)^2$ and (x_0, y_0) is the true cluster center, and, second, that the result is insenstive to the integral over y, i.e.,

$$\Psi_{\text{mod}}(\hat{x}) \approx 2W \int_0^W dx \, | f(\hat{x} - x, y) - f(\hat{x} + x, y) | . \quad (5)$$

The first approximation is the expression for a King model with $r \ll r_t$ (King 1962). The second approximation allows Ψ_{mod} to be expressed analytically. If the window is centered in the y-direction (which can be done, since the center may be estimated approximately to begin with), then it is clear that Ψ_{mod} is insensitive to variations along the y-axis and the integrand in equation (3) is only weakly dependent on y. Performing the indicated integration yields

$$\Psi_{\text{mod}}(\hat{x}) = b_1 + b_2 \Bigg[2 \arctan(\delta) + \arctan\left(\frac{W}{r_c} - \delta\right) + \arctan\left(\frac{W}{r_c} + \delta\right) \Bigg] , \quad (6a)$$

where

$$\delta = \left| \frac{\hat{x} - x_0}{r_c} \right| . \quad (6b)$$

Using previously published estimates of the core radius, $\Psi(\hat{x})$ is least-squares fitted to $\Psi_{\text{mod}}(\hat{x})$, yielding one coordinate of the cluster center x_0. For most clusters the location of the cluster center can be determined to a fraction of a pixel, or $\lesssim 0''.25$ relative to the surrounding field.

An estimate of the uncertainty in this procedure can be obtained from the agreement between the two sets of axes chosen on each plate (i.e., axes between pixels and axes through pixel centers) as well as the agreement between independent plates. The results from the two sets of axes on the same plate typically agree to $\lesssim 0.1$ pixels ($\lesssim ''.05$). The agreement between independent plates is dependent on the astronometry of each plate and is comparable to the astrometric uncertainty given in Table 3. Since this is much larger than the internal uncertainties on the center determination from each plate (estimated from comparison of fits to the two sets of axes), we estimate the uncertainty in the center determination for a cluster by adding in quadrature the difference between measurements on two independent plates to the uncertainty in the astrometry of the secondary standards for that cluster.

f) Surface Brightness Profiles and the Core Radius

In order to determine the structural parameters of the cluster, the core and tidal radii, the cluster's surface brightness profile is needed. So that we may measure the surface brightness of the cluster out to radii $r \gtrsim 100''$, large areas of the plate around the cluster core were scanned at various sampling densities (Table 2); these scans undersample the outer regions of the cluster. Most clusters were scanned to radii of $\sim 10'$–$15'$; the larger clusters 47 Tuc and NGC 6712 were scanned to $\sim 25'$.

Once the cluster center has been determined from the inner-cluster scan, the surface brightness profile of the entire cluster can be constructed. In order to minimize the effect of single bright stars (which may be 10^3–10^4 times brighter than the diffuse cluster emission nearby), the plate density measurements are binned in logarithmically spaced annuli. This procedure is not as effective in deemphasizing bright stars in crowded regions, but the additional uncertainty is small compared with the sampling errors. The average plate density in each annulus is converted into an intensity measurement. The formal error assigned to the average density in each annulus is the quadratic sum of the rms scatter of the densities in the annulus about the mean density and of the estimated measurement errors for each pixel in the annulus. The former term is an estimate (Newell and O'Neil 1978) of the sampling errors (King 1966*b*) due to the finite number of stars in each annulus. The data from all scans of a given plate are combined into a single surface brightness profile that is well determined over much of the cluster; halo profiles are less well determined than core profiles.

A King model (King 1966*a*) is then fitted to the surface brightness profile derived from the binned data. The three parameters of the model [core radius r_c; concentration parameter $c \equiv \log (r_t/r_c)$, where r_t is the tidal radius; and relative central surface brightness f_0] are determined through a least-squares fit to the data. In practice, r_c and f_0 are allowed to vary freely, while we vary c only in steps of 0.125.

Care must be taken in comparing the mean surface brightness in an annulus $\langle f \rangle$, which is the quantity measured, to the surface brightness profile model, which predicts the surface brightness at a single radius. We have followed a procedure similar to those of King (1966*b*) and Illingworth and Illingworth (1976) by defining an effective radius

$$r_e = [\tfrac{1}{2}(r_1^2 + r_2^2)]^{1/2} , \quad (7)$$

such that r_e is the radius bisecting the area of the annulus with inner radius r_1 and outer radius r_2. Using a simple approximation for King model,

$$f(r) = k\{[1 + (r/r_c)^2]^{-1/2} - K\}^2 , \quad (8a)$$

$$k = f_0(1 - K)^{-2} , \quad (8b)$$

$$K = [1 + (r_t/r_c)^2]^{-1/2} \quad (8c)$$

(cf. eq. [14] of King 1962), we derive

$$\frac{f(r_e)}{\langle f \rangle} = \frac{(y_2 - y_1)\{[(y_2 + y_1)/2]^{-1/2} - K\}^2}{\ln (y_2/y_1) - 4K(y_2^{1/2} - y_1^{1/2}) + K^2(y_2 - y_1)} , \quad (9)$$

where $y_i = 1 + (r_i/r_c)^2$ for $i = 1, 2$ and K is given by equation (8c). This correction has been applied to all data where we have fitted King models to the observed surface brightness profile.

The surface brightness profile has two distinct regions. When the plate background was fitted, and the background due to plate fogging was removed, it was fitted to density variations across the entire plate. The background varies from the average background on small scales (e.g., scales the size of the cluster itself) because of uneven plate fogging and developing. This systematic error gives rise to an uncertainty in the intensity calibration and dominates the errors for surface brightness profile. For the inner regions of the cluster, where the intensity of each pixel was obtained from the linear portion of the characteristic curve, these errors give rise to a constant shift in log intensity and will not affect the determination of the core radius. (They will, however, affect the determination of the central surface brightness; we thus determine only the relative central surface brightness.) In the outer regions of the cluster,

where the intensity was obtained from the toe of the characteristic curve, the surface brightness profile may be distorted; this affects our determination of the tidal radius.

Because of the nature of the error terms, the surface brightness profile is fitted in two steps. First, the data are fitted to a King model plus a constant background. The inner few annuli are usually not fitted, in order to weight the fit toward the outer portions of the cluster. The best-fit model determines the plate backgrounds (as a function of concentration parameter c) allowed.

Second, the plate background and the concentration parameter are fixed to the best-fit values derived for the outer portions of the cluster. The data minus the adopted plate background (out to where the cluster surface brightness approaches the plate background) are then fitted to a King model and the core radius is determined. The concentration parameter is allowed to vary somewhat to verify that this is actually the best fit. A formal reduced χ^2 statistic is generated and is typically less than ~ 1.0, indicating that we have overestimated the errors. From χ^2 we calculate a formal 1 σ error bar on the core radius. When $\chi^2_{\min} \gtrsim 1.0$, we take the uncertainty in r_c to be those values of r_c for which $\chi^2 < \chi^2_{\min} + 1.0$. In cases where we have seriously overestimated the errors and $\chi^2_{\min} \ll 1.0$, we take the 1 σ uncertainty in r_c to be those r_c for which $\chi^2 < 2\chi^2_{\min}$. The final value of r_c is typically determined to $\lesssim 10\%$.

III. RESULTS: CLUSTER CENTERS AND CORE RADII

We have determined the optical centers and core radii of eight X-ray globular clusters. Our final results are presented in Table 4, along with estimates of the 1 σ uncertainties in the cluster centers and core radii. The cluster centers and core radii, as well as the positions of the globular cluster X-ray sources (from Grindlay *et al.* 1984), are shown in Figure 1 (Plates 1 and 2). In this section we discuss the analysis of data from individual clusters and compare our results with previous work.

Comparison of our center positions with the positions reported by Shawl and White (1980, 1984) for six of the eight clusters in our study (NGC 104, NGC 1851, NGC, 6441, NGC 6624, NGC 6712, NGC 7078) shows general agreement. However, the positions differ significantly ($\sim 4''$, or $> 2\ \sigma$) for three clusters (NGC 1851, NGC 6441, NGC 6624). We note that their technique of image blurring may be biased by individual bright giants in the cluster (their study used Palomar and ESO *B* images), and it is most sensitive to the distribution of the bulk of the light in the cluster, i.e., the halo. Since our center is weighted to the core of the cluster (our original objective was to determine the center of mass of the core), a possible nonconcentricity between the cluster's core and halo could also account for the differences. Further work is called for to resolve these discrepancies.

Previous measurements of core radii of X-ray globular clusters by eye estimates (Peterson and King 1975) or star counts (Bahcall 1976; Bahcall and Hausman 1976) have uncertainties up to 50%–70% of the core radius. Previous photometric measurements of core radii (e.g., Illingworth and Illingworth 1976; Canizares *et al.* 1978; Malkan, Kleinmann, and Apt 1980) yield measurements of r_c to $<15\%$–30%. However, they are limited by the accuracy with which the cluster center can be estimated at the telescope and, in some cases, by the resolution of the apertures used. Comparison of our core radii with those determined by photometric means, however, shows general agreement.

In Figures 2 and 3 we show the surface brightness profiles for the seven clusters for which we determined a surface brightness profile. We have plotted the surface brightness for each annulus at the effective radius of the annulus, as discussed in § II*f*. We have also applied the appropriate correction to the mean surface brightness in the annulus to convert it into a local surface brightness. The point response function, or stellar disk seeing profile, is indicated for each cluster by the dashed curve. In the remainder of this section, we discuss the analysis of each cluster individually.

a) NGC 104 = 47 Tuc

47 Tuc (= NGC 104) is located near the south ecliptic pole ($\delta \approx -72°$). In this region of the sky the positions of individual stars reported in the *SAO Catalogue* are poorly determined. The rms error is $\sim 2''.5$ for the *SAO Catalogue* positions of stars near 47 Tuc (Shawl and White 1984). Using ~ 15 primary standards and ~ 9 secondary standards, we have determined the position of the cluster center on each plate to $\sim 1''$. The two positions differ by $\sim 2''.1$, and an average uncertainty of $1''.3$ is assigned to the mean position for the cluster center. The core radius is well determined with our data, and our value agrees with the value obtained by Illingworth and Illingworth (1976). Note that we find no evidence for any central cusp or departure from a simple King model in the cluster core, even though

TABLE 4

GLOBULAR CLUSTER CENTERS AND CORE RADII

GLOBULAR CLUSTER	CLUSTER CENTER R.A.	CLUSTER CENTER Decl.	1 σ (arcsec)	CORE RADIUS (arcsec)	ADOPTED CORE RADIUS (arcsec)	APPROXIMATE CONCENTRATION
NGC 104 = 47 Tuc	$00^h21^m53^s.16$	$-72°21'29''.9$	1.3	23.6 ± 1.3	...	2.5:
NGC 1851	05 12 28.03	−40 06 11.4	0.5	4.6 ± 0.7	5.9 ± 0.7	1.8
Terzan 2	17 24 19.95	−30 45 36.7	1.0	6.5 ± 1.4	...	1.3:
Liller 1	17 30 06.61	−33 21 19.7	1.0	3.5 ± 0.2	...	1.6:
NGC 6441	17 46 48.75	−37 02 15.8	0.5	8.2 ± 0.3	...	1.6
NGC 6624	18 20 27.56	−30 23 15.6	0.6	5.2 ± 0.5	...	2.4
NGC 6712	18 50 20.78	−08 46 06.5	5.7	...	49.0 ± 5.0	...
NGC 7078 = M15	21 27 33.40	11 56 48.9	0.5	5.5 ± 1.0	...	2.1:

NOTE.—Positions listed are epoch 1950.0. The listed errors in position are the 1 σ error radii in arcseconds. The cluster core radii and their 1 σ errors are in arcseconds. Adopted core radii are explained in the text. Concentration parameters [$\equiv \log (r_t/r_c)$] are indicative only, owing to the possible systematic errors introduced in the data analysis process (see text). Uncertainties in the concentration parameter are $\sim \pm 0.3$ when indicated by a colon (:), ± 0.2 otherwise.

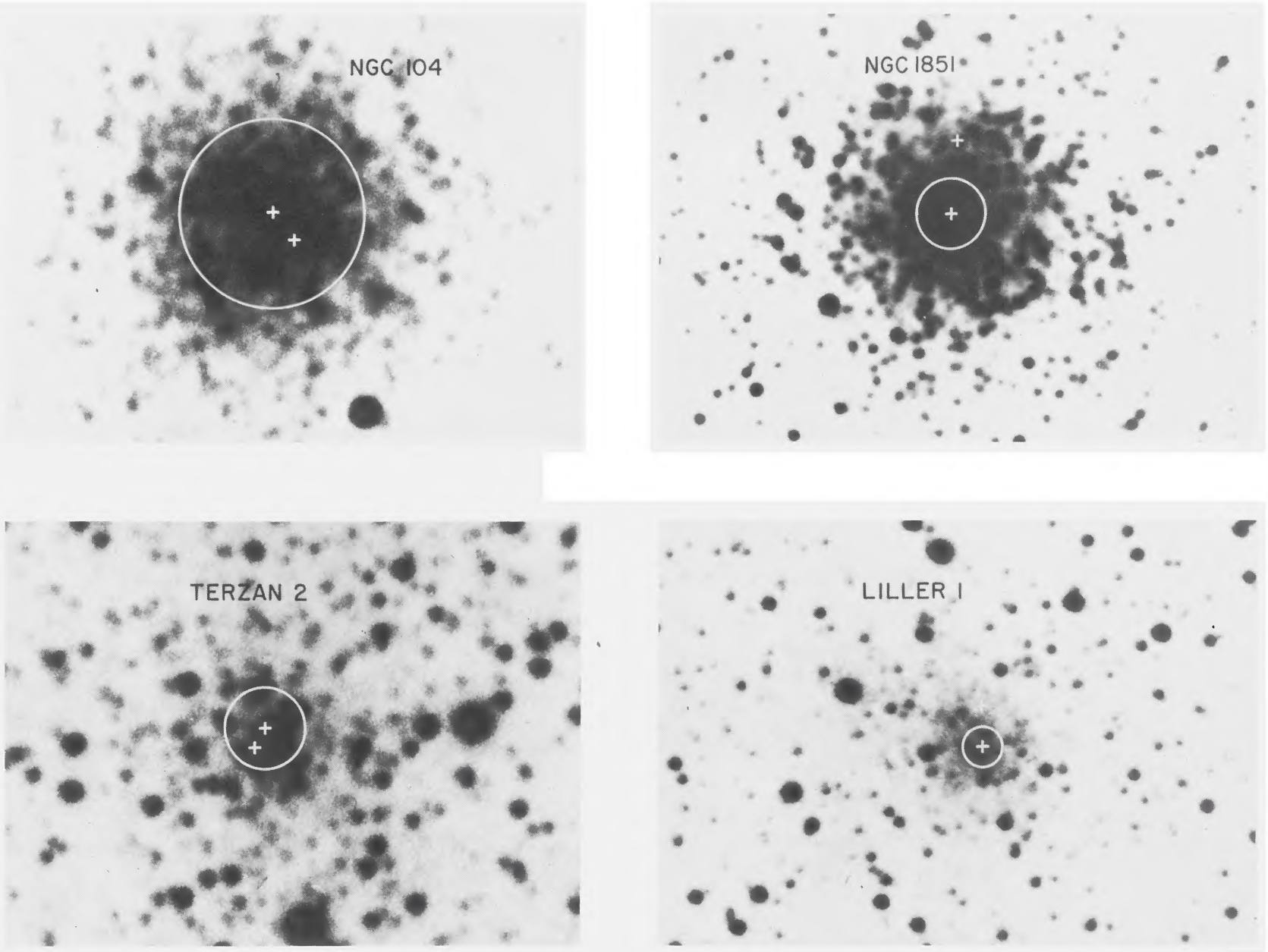

FIG. 1.—Centers and core radii of eight X-ray globular clusters. Superposed on *U* or *I* images from our 4 m plates of each globular cluster are the cluster center and core radius. The scale is given by the size of the core radius (with references to Table 4). The location of the X-ray source in each cluster, from Grindlay *et al.* (1984), is also indicated.

HERTZ AND GRINDLAY (*see* page 99)

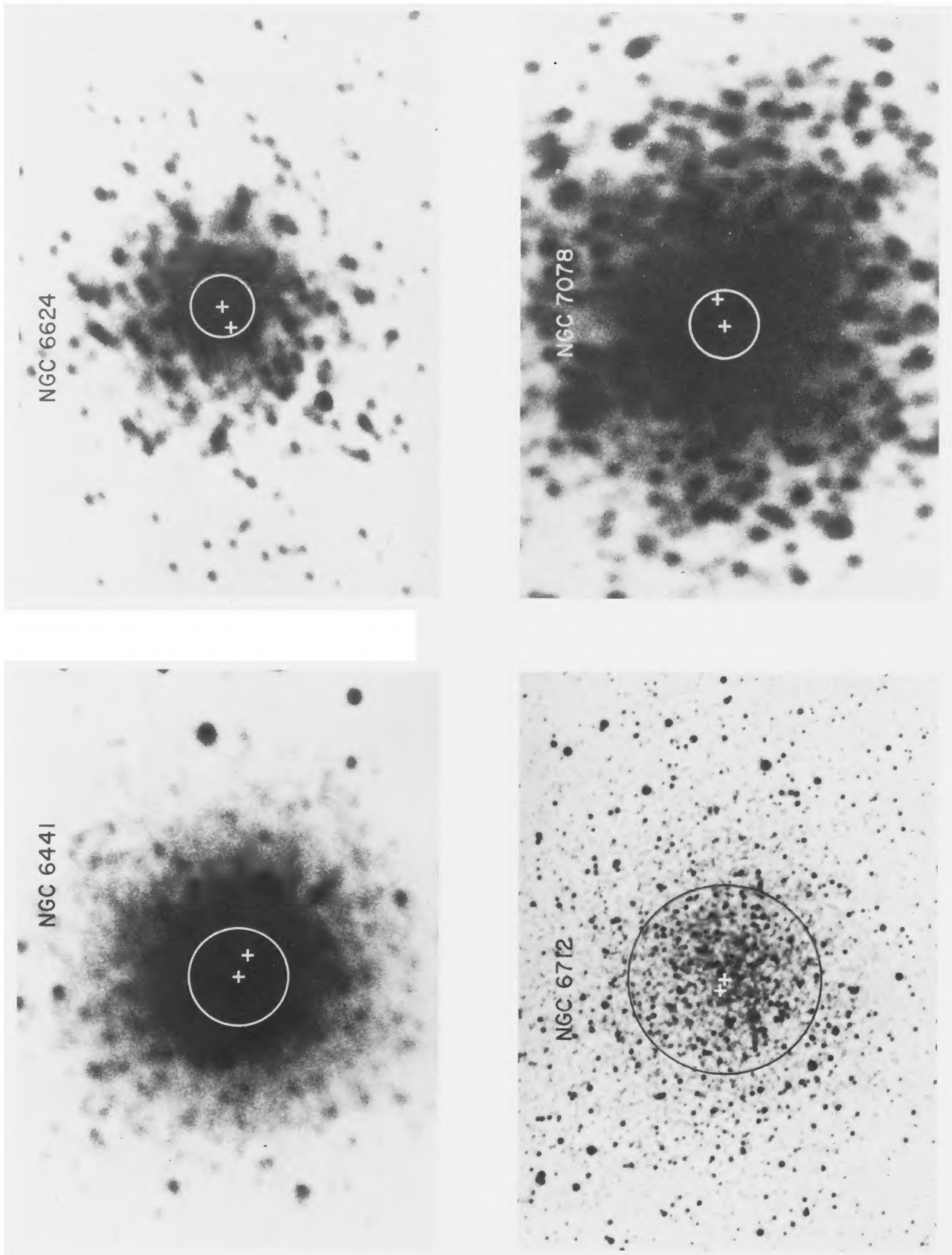

FIG. 1.—*Continued*

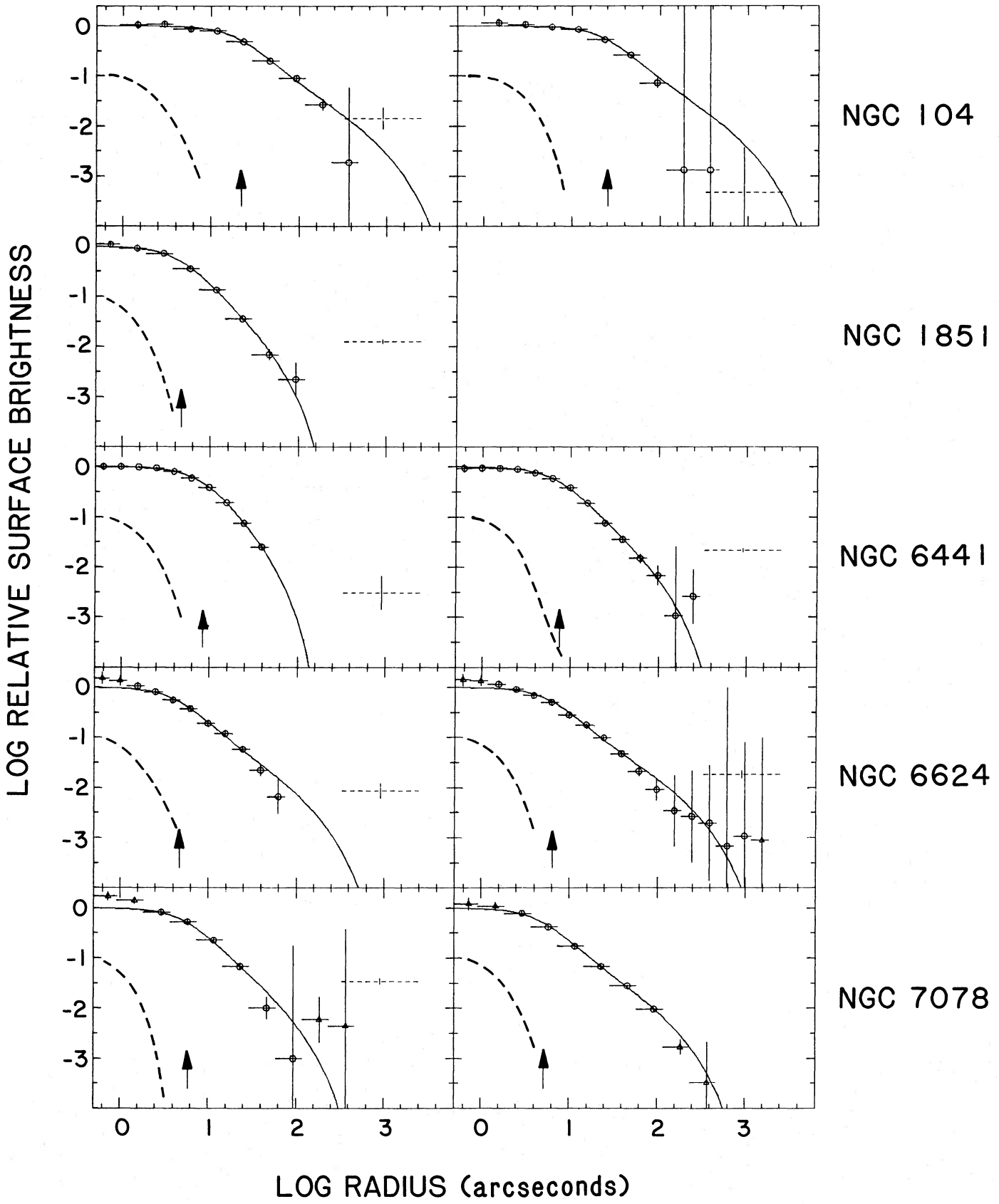

FIG. 2.—Surface brightness profiles for five X-ray globular clusters. The solid line is the best-fit King model (see Table 4). Representative error bars are shown for each data point; triangles indicate data points which were not included in the determination of the best-fit King model. The horizontal dashed line is the fitted plate and sky background which has been subtracted from each profile. The dashed profile is the point-source response for each image normalized to 0.1 times the central surface brightness of the cluster. *Top to bottom:* the five clusters shown are 47 Tuc (NGC 104), NGC 1851, NGC 6441, NGC 6624, and M15 (NGC 7078); measurements from *B* plates are on the left, *U* plates on the right.

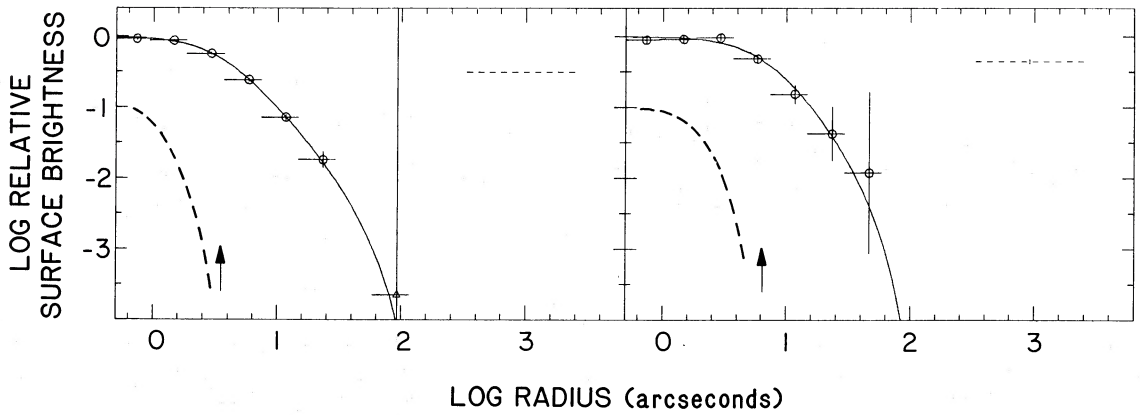

FIG. 3.—Surface brightness profiles for two X-ray globular clusters. The data are from near-infrared *I* plates of Liller 1 (*left*) and Terzan 2 (*right*). Other details as in Fig. 2.

the velocity dispersion studies of Da Costa and Freeman (1984) show evidence for dark matter in 47 Tuc. Our best-fitted concentration parameter ($c \gtrsim 2.5$ on both plates) is inconsistent with the value 2.03 ± 0.04 obtained by Illingworth and Illingworth. Because of 47 Tuc's large size and apparent brightness, the background is poorly determined on our plates; this causes the outer portions of the cluster to be distorted. For these reasons, our determination of c is very uncertain.

b) NGC 1851

The center of NGC 1851 is well determined, and there is no apparent difference in the positions of the cluster center found on the *U* and *B* plates. The central core regions of the *U* image are saturated, so the core radius cannot be determined from that plate; the saturated bins are not included in the determination of the cluster center. This leaves only a single measurement of r_c. As our result is consistent with that of Illingworth and Illingworth (1976), we adopt the mean of these two measurements as the core radius. Our determination of c agrees with that of Illingworth and Illingworth. Note that our surface brightness profile does not show the smooth dip in brightness at radii of $\sim 10''$–$15''$ as reported by DK. The size of the radial bins used by DK in determining the surface brightness profile of NGC 1851 is smaller than the point response of their plates (as derived from a stellar profile); thus the several bins which contribute to the smooth dip in the profile are not independent. The dip could be due to a local (negative) fluctuation in the number of bright giants, and the size of the dip appears to be comparable to the sampling errors for NGC 1851. Our logarithmically spaced radial bins are larger than DK's, and it is therefore likely that we have averaged over the dip in the cluster's profile.

c) Terzan 2

A single, deep *I* plate was obtained of Terzan 2. The center is well determined, and the surface brightness profile is well fitted by a King model. The value of r_c derived agrees with that of Malkan, Kleinmann, and Apt (1980), although our surface brightness profile has much better resolution and hence our uncertainties are smaller.

d) Liller 1

A single, deep *I* plate was also obtained of Liller 1, the obscured globular cluster (Liller 1977) associated with the rapid burster (MXB 1720−335). The center is well determined, although difficulties in identifying the secondary standards on the ESO plate resulted in only five usable secondary standards. The cluster appears very clumpy on our 4 m plate (as does Terzan 2), presumably because of the enhanced effects of bright giants in the near-infrared. There is not a significant clump at the cluster center.

We obtained an excellent fit of a King model to the surface brightness profile. Leaving the central two bins out of the fit to a King model showed that there is no central excess in the cluster. Our determination of the core radius ($3''.5 \pm 0''.2$) is significantly smaller than that of Kleinmann, Kleinmann, and Wright (1976; $6''.5 \pm 0''.5$) and marginally smaller than that of Malkan, Kleinmann, and Apt (1980; $7''.0 \pm 2''.0$). The difference is due to the resolution of the data. The smooth and diffuse nature of the globular cluster allowed us to measure the central portions of the cluster with annuli as small as $1''$. The larger central apertures in Kleinmann, Kleinmann, and Wright ($\sim 9''$) and Malkan, Kleinmann, and Apt ($\sim 3''$) account for the difference. In addition, both groups centered their apertures on the peak of emission; because of the cluster's clumpy nature, they may have missed the cluster center by a significant amount.

e) NGC 6441

NGC 6441 is the perfect test cluster, and we used it to test all of our analysis software before tackling other, less well-behaved clusters. NGC 6441 has a surface brightness profile which is almost exactly fitted by a King model, with no lumps, bumps, or clumps to complicate the fit. The cluster center is well determined on two plates, with excellent agreement between the two. The core radius was also determined from two plates, and the agreement is good between the two as well as with Illingworth and Illingworth (1976). Our determination of the concentration parameter is also in good agreement with Illingworth and Illingworth.

f) NGC 6624

NGC 6624 has been reported to have a bright clump of stars at or near its center (star B of Canizares *et al.* 1978), so we took care not to be unduly influenced by its presence. We determined the cluster center in three ways: the standard technique described above, finding the peak flux in the cluster image, and removing the central $5''$ of the cluster from the MSM foldings. All three techniques gave consistent results; we have reported the position from the standard MSM foldings in Table 4. A King model did not fit the surface brightness profile well unless

we left the central two bins (1″ radius) out of the fit. In that case, the fit is excellent and the core radius determined agrees well with those of Canizares *et al.* (1978) and Bahcall (1976). The excess light in the core of the cluster, which is visible on both the *U* and *B* plates, is discussed further in § IV.

g) NGC 6712

NGC 6712 is a diffuse globular cluster (Peterson and King 1975), uncharacteristically diffuse for an X-ray globular cluster (Grindlay 1977). Individual bright stars dominate the diffuse emission on our 4 m plates. The noise in the measure of symmetry Ψ is large compared with the depth of the minimum at the center and we cannot determine the location of the center accurately. Our uncertainty is large ($\sim 10''$ on a single plate), and is $\sim 5''$ on the mean position. Since we did not detect the diffuse emission with the cluster binned, we are unable to determine the surface brightness profile and core radius of NGC 6712. We have used the value of 49″ given by Peterson and King (1975) and adopted a conservative uncertainty of 5″. Note that this value is consistent with the recent determination of $r_c \approx 41''$ by Kron, Hewitt, and Wasserman (1984).

h) NGC 7078 = M15

M15 (= NGC 7078) is another well-behaved cluster, and we had no problem determining the position of the center with arcsecond accuracy on both plates. We ignored the central 5″ of the cluster in determining the position of the center because of previous reports of excess light at the cluster core (King 1975; Leroy, Aurière, and Laques 1976; Newell, Da Costa, and Norris 1976). A King model fitted M15 considerably better when the central two bins were excluded from the fit, thus confirming the central excess light. We discuss the excess in § IV, and note here that our determination of r_c is smaller than those determined using star counts (Peterson and King 1975; Bahcall, Bahcall, and Weistrop 1975; Aurière and Cordoni 1981). The two M15 plates were scanned during a different PDS run from those of the other clusters, and there is considerable hysteresis in the digitized image. For this reason we doubled the formal error of 0.″5 for the core radius.

IV. PROBING THE CORE: CENTRAL CUSPS IN TWO CLUSTERS

In Figures 2 and 3 we present the surface brightness profiles and best-fit King (1966*a*) models to those profiles for seven of the eight clusters studied here. (As previously noted, we could not derive a surface brightness profile for NGC 6712 because of its diffuse nature.) Five of the X-ray globular clusters are well fitted by King models; however, two, NGC 6624 and M15 (= NGC 7078), exhibit cusps at their cores. We searched for cusps in all clusters by fitting King models to the surface brightness profile without including the central few radial bins in the fit. We then looked for a significant residual between the King model which best fitted the shoulder of the surface brightness profile and the central few bins. Only in NGC 6624 and M15 did we observe such a residual (Fig. 4). In both clusters the cusp is detectable only within ~ 0.4 core radii of the cluster center, and it is apparently broader than the stellar point response function (cf. Fig. 2).

The cusp, or excess central surface brightness, at the core of M15 has long been noted (e.g., King 1975), and we provide additional confirmation of its existence here. It has been modeled as a central black hole (Newell, Da Costa, and Norris 1976; Bahcall, Bahcall, and Weistrop 1975), as a clump of neutron stars (Illingworth and King 1977) or other faint stars (Aurière and Cordoni 1981), and as an example of a globular cluster either undergoing or having completed core collapse. However, in previous discussions (except for DK), it has not been possible to state whether the cusp is precisely at the cluster center and therefore dynamically interesting. Our measurements show this to be the case.

We have previously reported the excess central surface brightness at the center of NGC 6624 (Grindlay 1983), and it has recently been confirmed by DK. An apparent brightness peak in the core of NGC 6624 had been qualitatively noted by several observers (Bahcall 1976; and Harvel and Martins 1977;

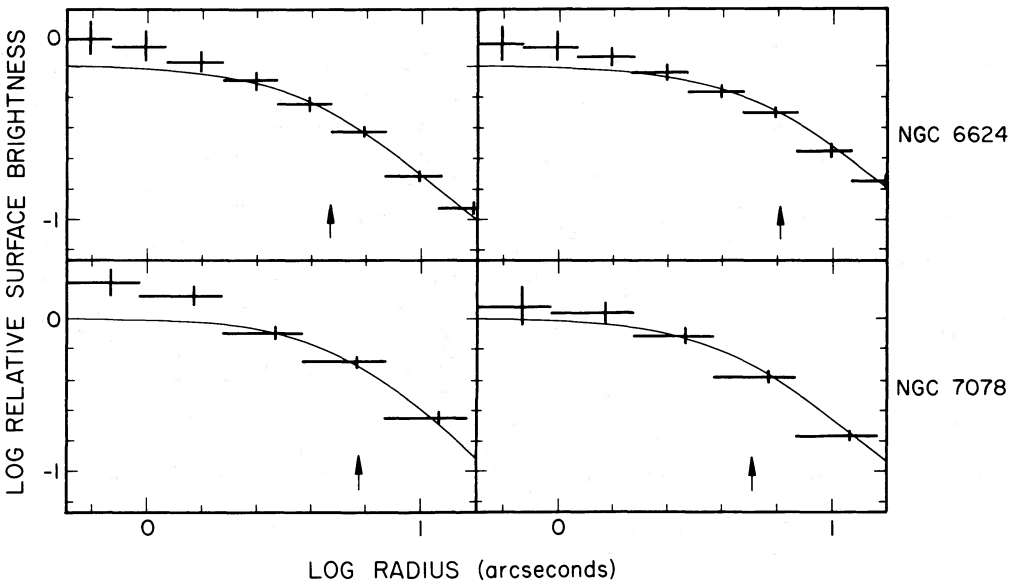

FIG. 4.—Surface brightness profiles for NGC 6624 and M15 (NGC 7078) showing the excess central surface brightness over the best-fit single-mass King model. These are an expansion of the profiles in Fig. 2; see Fig. 2 caption for details.

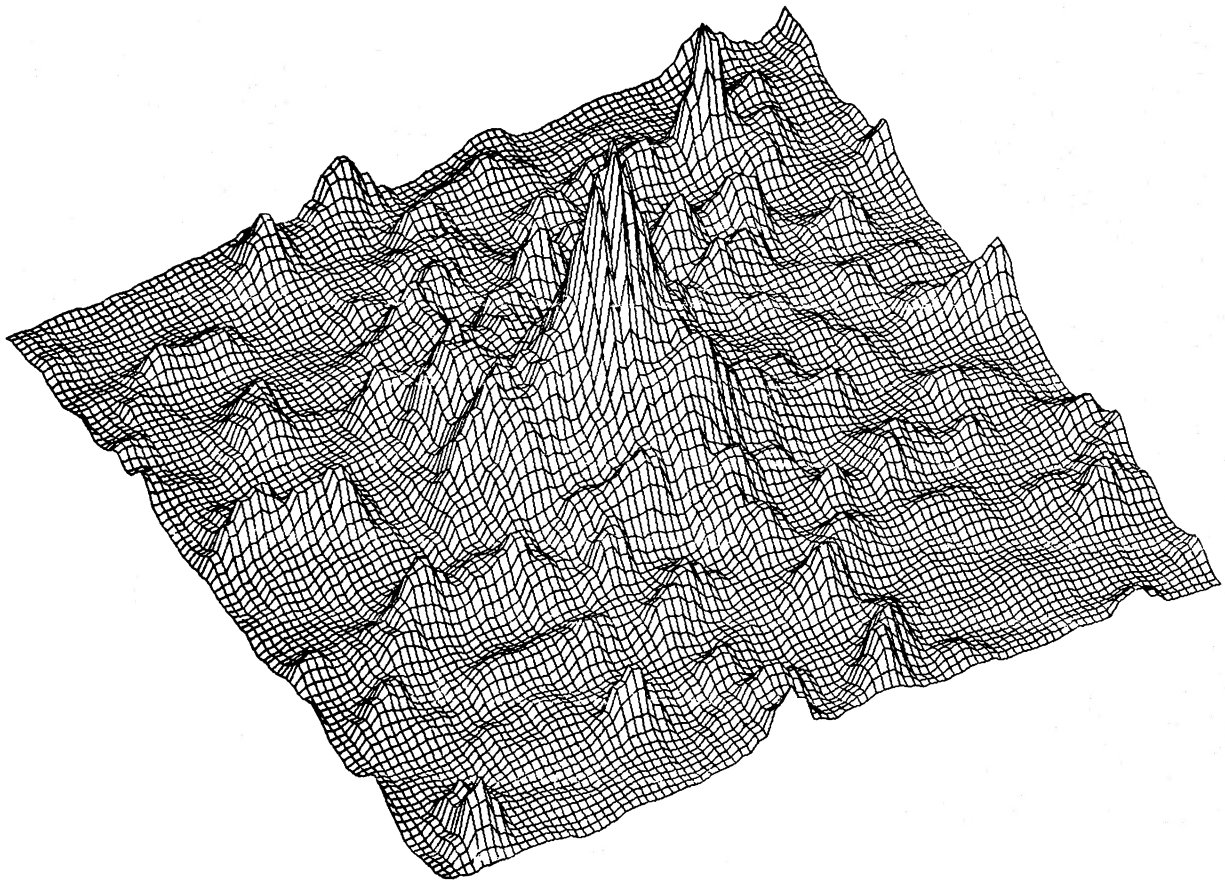

FIG. 5.—Three-dimensional representation of NGC 6624. This linear map of NGC 6624 is from a 30 minute exposure in U; north is to the lower right, east is to the upper right. The entire image is approximately 50″ × 50″ in size; each pixel is ~0″.5.

Canizares *et al.* 1978) and has been previously interpreted as a clump of luminous giant stars (Canizares *et al.* 1978). Once again, the earlier reports were unable to show that the excess light peaked at the true center of the cluster.

Both of these clusters are X-ray globular clusters. DK have recently reported excess surface brightness at the cores of at least two non–X-ray clusters (NGC 6681 = M70, NGC 7099 = M30). It is not clear how widespread this phenomenon is, or whether it is correlated with other properties of globular clusters. However out of the seven X-ray (this work) and four additional highly concentrated (DK) globular clusters for which surface brightness profiles have been determined with sufficient resolution to detect excess central surface brightness, at least four are reported to have such an excess.

In order to investigate further the shape of the excess in NGC 6624, we performed a two-dimensional FFT of the cluster image. We then truncated the resulting power spectrum so as to separate the unresolved stellar components of the image from the diffuse emission of unresolved stars in the globular cluster. In Figure 5 we show the original U plate image of NGC 6624, and in Figure 6 we show the image sorted by a Fourier filter. The cutoff frequency corresponds to a wavelength of 2″.9, larger than the ~1″.7 FWHM of the point-source response for this image. If this cluster had no central cusp, it would be fairly simple to determine the center of the cluster from the filtered cluster image in Figure 6*b*. Any center determination, other than the maximum-symmetry method or a similar method (e.g., that of DK), will locate the center of the cusp; this may or may not be the cluster center. Since there is not an excessively bright stellar image at the cluster center in the high-frequency image (Fig. 6*a*), the peak at the center of the cluster image remains in the cluster image (Fig. 6*b*) and was not filtered out. This indicates that the peak in the core of NGC 6624 is resolved and is not due to a single bright star (although the excess light in Fig. 4 is not significantly broader than the seeing disk profile). It must be a collection of stars representing a luminosity excess; it is not clear from this exercise whether these stars represent an excess of mass as well.

We have summed up the excess luminosity in the central three annuli of our surface brightness profile of NGC 6624. These annuli contain the central 2″ (radius) of the cluster. We have detected an excess of 0.18 ± 0.09 mag of flux averaged over both U and B plates. All six annuli included in the summation show an excess over the best-fit King model. However, the uncertainties (dominated by sampling errors in annuli this small) are such that a meaningful color for the excess cannot be derived. Nevertheless, the excess light appears bluer in color. Canizares *et al.* (1978) report for NGC 6624 that the cluster center (their star B) may be bluer than the rest of the cluster, and Aurière and Cordoni (1981) indicate a dearth of red giants at the core of M15.

The large sampling errors on our inner annuli prevent us from confirming a previous report that the surface brightness profile for the inner regions of NGC 6624 is a power law with a slope of -1 (DK). Our data are consistent with such a slope within the inner 10″ of the cluster. However, whereas the DK

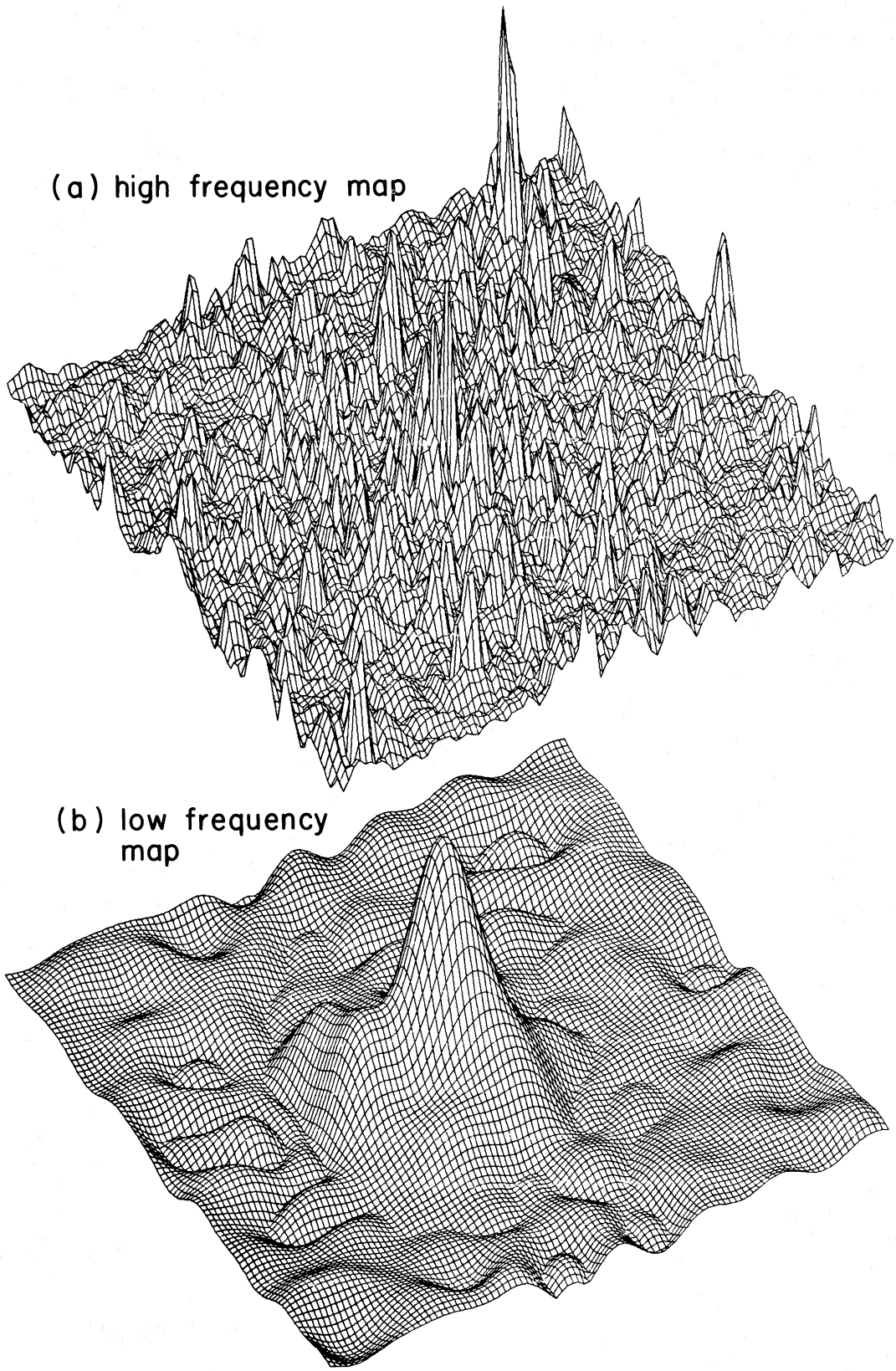

FIG. 6.—Fourier filtered images of NGC 6624. The image in Fig. 5 has been Fourier filtered into (*a*) high-frequency (bright star) and (*b*) low-frequency (diffuse light) images. The images were separated at a frequency corresponding to a wavelength of approximately 3″. Note that the sharp peak in the cluster center is present in the low-frequency image, although stars have been suppressed. This indicates that the central component is resolved. Each figure has been scaled independently for display purposes.

surface brightness profile is consistent with such a slope out to radii of $\sim 20''$ for their data (which extend out to only $\sim 30''$), our results (Fig. 2) show that a standard King model (with slope of -2) adequately describes the cluster surface brightness out to $\sim 100''$ radii.

V. SEARCH FOR COLOR DEPENDENCE IN GLOBULAR CLUSTER STRUCTURE

We have conducted the first globular cluster surface brightness study in U and B which has both the sensitivity and the resolution to detect possible color dependence in globular cluster properties. We have detected none; thus different populations of stars within globular clusters, which may be expected to have different colors and to have undergone mass segregation as the cluster relaxed, are distributed symmetrically about the same center and have similar radial distributions. This could indicate that the bulk of the light in both U and B comes from the same population of stars. These results are in agreement with the recent summary of Peterson (1984, and results quoted therein).

The centers of five X-ray globular clusters have been measured in both U and B (see Table 5). We detected no significant difference in the U- and B-determined centers. Any difference could indicate an unrelaxed system between the giants and main-sequence stars, which have different colors. The absence of such a difference indicates that the dynamical center of the cluster can be unambiguously defined and measured.

In addition, we have measured the core radii of four globular clusters in more than one color. For comparison, we show our U and B core radii measurements in Table 6, along with core radii determined from V observations by Illingworth and Illingworth (1976) and Canizares *et al.* (1978). Again we note that there is no significant difference as a function of color. Thus a single-mass-component King model is adequate for our purposes.

A more stringent test for color differences can be conducted by making use of Fourier filtered images. We expect that when King models are fitted to the separate images derived from the Fourier deconvolution, the "high- frequency" cluster (bright giants) may have a smaller core radius than the "low-frequency" cluster (more diffuse main-sequence stars). This test will be applied to a larger sample of globular clusters, which we are currently obtaining.

VI. DISCUSSION

We have conducted a sensitive study of the structure of eight X-ray globular clusters. Our purpose has been primarily to determine the centers and core radii of these clusters with good precision. The cluster centers and core radii were derived with high enough precision to allow the X-ray source mass to be determined (Grindlay *et al.* 1984) and to stimulate a future study of a much larger sample of globular clusters in the Galaxy. We have also examined the validity of King model fits to the data and have found that a single-component King model is a good fit to the structure of these clusters, with two notable exceptions. These exceptions are the excess light (or central cusps) at the center of NGC 6624 and M15. The existence of these central excesses may be uncorrelated with the presence of bright X-ray sources (DK), although it is likely that the higher stellar densities in cusps result in a greater production of tidal capture binaries, only a fraction of which are detectable at any one time as high-luminosity X-ray sources. Thus the assumption of a relaxed, isothermal system described by a single mass component is acceptable (on average) for determining the mean mass of the globular cluster X-ray sources (Grindlay *et al.* 1984).

The central cusps in NGC 6624 and M15, however, indicate simple single-mass models, and pre–core-collapse evolutions are not adequate to describe these clusters completely. The central excess light may be due either to an enhanced central potential from a collapsing subcore of heavy remnants or to excess light from a central population of binaries (e.g., blue straggler stars). Higher resolution studies, both spatial and spectral, are needed.

The questions which these studies raise go beyond the structure of X-ray globular clusters. We are therefore obtaining CCD images of other concentrated globular clusters, primarily southern hemisphere clusters. The use of a CCD instead of photographic photometry will improve our photometric capabilities and allow us to search more sensitively for central excesses in other clusters. These studies will once again be done in U and B, except for heavily reddened clusters. We will also be able to study departures from King models and further constrain any color-dependent differences in cluster structure. Finally, the FFT techniques will be applied to a larger sample of clusters for a better understanding of the distributions of resolved and unresolved sources of light.

TABLE 5

DIFFERENCE IN GLOBULAR CLUSTER CENTERS ON U AND B PLATES

Cluster	Δ(R.A.)	Δ(Decl.)	Δ(Total)
47 Tuc	−1.1	+1.8	2.1 ± 1.8
NGC 1851	+0.3	−0.2	0.4 ± 0.7
NGC 6441	+0.2	−0.2	0.3 ± 0.7
NGC 6624	+0.9	−0.6	1.1 ± 0.7
NGC 6712	+5.6	+1.5	5.8 ± 8.1
M15	−0.3	−0.3	0.4 ± 0.7

NOTE.—Differences are in arcseconds and are in the sense U plate minus B plate. Uncertainties are 1 σ errors in the differences.

TABLE 6

DIFFERENCES IN GLOBULAR CLUSTER CORE RADII AS A FUNCTION OF COLOR

Cluster	V	B	U
47 Tuc	24.4 ± 2.3[a]	22.2 ± 1.2	25.4 ± 1.4
NGC 1851	7.2 ± 0.7[a]	4.6 ± 0.7	...
NGC 6441	9.1 ± 0.8[a]	8.4 ± 0.3	7.4 ± 0.5
NGC 6624	5.0 ± 0.5[b]	4.7 ± 0.4	6.4 ± 0.6
M15	...	5.9 ± 0.5	5.1 ± 0.2

NOTE.—Core radii and 1 σ uncertainties are in arcseconds.
[a] Illingworth and Illingworth 1976.
[b] Canizares *et al.* 1978.

We thank Ed Turner at Princeton and Jin-Fuw Lee at Yale for assistance in using their respective PDS systems. We also thank Brian Flannery for providing numerical King models, Harriet Griesenger for help with the CfA microdensitometer, Martha Liller for obtaining U and B plates of NGC 1851 and M15, and Ivan King for discussions of MSM. This work was supported in part by NASA contract NAS8-30751.

REFERENCES

Aurière, M., and Cordoni, J.-P. 1981, *Astr. Ap.*, **100**, 307.
Bahcall, J. N., Bahcall, N. A., and Weistrop, D. 1975, *Ap. Letters*, **16**, 159.
Bahcall, J. N., and Ostriker, J. P. 1975, *Nature*, **256**, 23.
Bahcall, J. N., and Wolf, R. A. 1976, *Ap. J.*, **209**, 214.
Bahcall, N. A. 1976, *Ap. J.* (*Letters*), **204**, L83.
Bahcall, N. A., and Hausman, M. A. 1976, *Ap. J.* (*Letters*), **207**, L181.
Canizares, C. R., Grindlay, J. E., Hiltner, W. A., Liller, W., and McClintock, J. E. 1978, *Ap. J.*, **224**, 39.
Clark, G. W. 1975, *Ap. J.* (*Letters*), **199**, L143.
Da Costa, G. S., and Freeman, K. C. 1984, in *IAU Symposium 113, Dynamics of Star Clusters*, ed. P. Hut and J. Goodman (Dordrecht: Reidel), in press.
Djorgovski, S., and King, I. R. 1984, *Ap. J.* (*Letters*), **277**, L49 (DK).
Giacconi, R., Murray, S., Gursky, H., Kellogg, E., Schreier, E., Matilsky, T., Koch, D., and Tananbaum, H. 1974, *Ap. J. Suppl.*, **27**, 37.
Grindlay, J. E. 1977, *Highlights Astr.*, **4**, 111.
———. 1983, *Adv. Space Res.*, **2**, 133.
Grindlay, J. E., and Hertz, P. 1981, *Ap. J.* (*Letters*), **247**, L17.
Grindlay, J. E., Hertz, P., Steiner, J. E., Murray, S. S., and Lightman, A. P. 1984, *Ap. J.* (*Letters*), **282**, L13.
Harvel, C. A. and Martins, D. H. 1977, *Ap. J.* (*Letters*), **213**, L49.
Hertz, P. 1984, *Proc. Internat. Symposium on X-Ray Astronomy* (Bologna), ed. M. Oda and R. Giacconi (Tokyo: ISAS), p. 85.
Hertz, P., and Grindlay, J. E. 1983, *Ap. J.* (*Letters*), **267**, L83.
Hertz, P., and Wood, K. S. 1985, *Ap. J.*, **290**, 171.
Illingworth, G., and Illingworth, W. 1976, *Ap. J. Suppl.*, **30**, 227.
Illingworth, G., and King, I. R. 1977, *Ap. J.*, **218**, L109.
King, I. R. 1962, *A.J.*, **67**, 471.
———. 1966*a*, *A.J.*, **71**, 64.
King, I. R. 1966*b*, *A.J.*, **71**, 276.
———. 1975, in *IAU Symposium 69, Dynamics of Stellar Systems*, ed. A. Hayli (Dordrecht: Reidel), p. 99.
———. 1980, in *Globular Clusters*, ed. D. Hanes and B. Madore (Cambridge: Cambridge University Press), p. 249.
Kleinmann, D. E., Kleinmann, S. G., and Wright, E. L. 1976, *Ap. J.* (*Letters*), **210**, L83.
Kron, G. E., Hewitt, A. V., and Wasserman, L. H. 1984, *Pub. A.S.P.*, **96**, 198.
Leroy, J. L., Aurière, M., and Laques, P. 1976, *Astr. Ap.*, **53**, 227.
Lewin, W. H. G., and Joss, P. C. 1981, *Space Sci. Rev.*, **28**, 3.
———. 1983, in *Accretion Driven Stellar X-Ray Sources*, ed. W. H. G. Lewin and E. P. J. van den Heuvel (Cambridge: Cambridge University Press), p. 41.
Lightman, A. P., and Grindlay, J. E. 1982, *Ap. J.*, **262**, 145.
Lightman, A. P., Hertz, P., and Grindlay, J. E. 1980, *Ap. J.*, **241**, 367.
Liller, W. 1977, *Ap. J.* (*Letters*), **213**, L21.
Malkan, M., Kleinmann, D. E., and Apt, J. 1980, *Ap. J.*, **237**, 432.
Newell, B., Da Costa, G. S., and Norris, J. 1976, *Ap. J.* (*Letters*), **208**, L55.
Newell, B., and O'Neil, E. J., Jr. 1978, *Ap. J. Suppl.*, **37**, 27.
Peterson, C. J. 1984, in *IAU Symposium 113, Dynamics of Star Clusters*, ed. P. Hut and J. Goodman (Dordrecht: Reidel), in press.
Peterson, C. J., and King, I. R. 1975, *A.J.*, **80**, 427.
Schweizer, F., Gonzalez, R., and Saa, O. 1980, *CTIO Newsletter*, No. 3, p. 1.
Shawl, S. J., and White, R. E. 1980, *Ap. J.* (*Letters*), **239**, L61.
———. 1984, *Bull. AAS*, **16**, 501.
Smithsonian Astrophysical Observatory, 1966, *SAO Catalogue* (Washington: Smithsonian Institution).
Tsubaki, T., and Engvold, O. 1975, *AAS Photo-Bull.*, **2**, 17.

JONATHAN E. GRINDLAY: Harvard-Smithsonian Center for Astrophysics, 60 Garden Street, Cambridge, MA 02138

PAUL HERTZ: Code 4121.5, US Naval Research Laboratory, Washington, DC 20375